Vesicle capture, not delivery, scales up neuropeptide storage in neuroendocrine terminals

Dinara Bulgari[a], Chaoming Zhou[a], Randall S. Hewes[b], David L. Deitcher[c], and Edwin S. Levitan[a,1]

[a]Department of Pharmacology and Chemical Biology, University of Pittsburgh, Pittsburgh, PA 15261; [b]Department of Biology, University of Oklahoma, Norman, OK 73019; and [c]Department of Neurobiology and Behavior, Cornell University, Ithaca, NY 14853

Edited by Eve Marder, Brandeis University, Waltham, MA, and approved January 24, 2014 (received for review November 26, 2013)

Neurons vary in their capacity to produce, store, and release neuropeptides packaged in dense-core vesicles (DCVs). Specifically, neurons used for cotransmission have terminals that contain few DCVs and many small synaptic vesicles, whereas neuroendocrine neuron terminals contain many DCVs. Although the mechanistic basis for presynaptic variation is unknown, past research demonstrated transcriptional control of neuropeptide synthesis suggesting that supply from the soma limits presynaptic neuropeptide accumulation. Here neuropeptide release is shown to scale with presynaptic neuropeptide stores in identified *Drosophila* cotransmitting and neuroendocrine terminals. However, the dramatic difference in DCV number in these terminals occurs with similar anterograde axonal transport and DCV half-lives. Thus, differences in presynaptic neuropeptide stores are not explained by DCV delivery from the soma or turnover. Instead, greater neuropeptide accumulation in neuroendocrine terminals is promoted by dramatically more efficient presynaptic DCV capture. Greater capture comes with tradeoffs, however, as fewer uncaptured DCVs are available to populate distal boutons and replenish neuropeptide stores following release. Finally, expression of the Dimmed transcription factor in cotransmitting neurons increases presynaptic DCV capture. Therefore, DCV capture in the terminal is genetically controlled and determines neuron-specific variation in peptidergic function.

nerve terminal | secretory granule | neurotransmission | LDCV

The complex function of the brain relies on the functional diversity of individual neurons. One key parameter that differentiates neurons is their capacity to release small-molecule transmitters packaged in small synaptic vesicles (SSVs) and bioactive peptides (i.e., neuropeptides, neurotrophins, and enzymes) packaged in large dense-core vesicles (DCVs). For example, synaptic terminals that are specialized for fast transmission typically have boutons with many SSVs and few DCVs, the latter of which support cotransmission. However, there are also specialized neurons that have terminals that are packed with DCVs. Such neuroendocrine terminals are often linked to massive episodic neuropeptide release that triggers important behaviors such as egg laying in *Aplysia* or ecdysis in insects (1). The mechanism that accounts for variation in presynaptic neuropeptide storage (i.e., the number of DCVs in a terminal) in cotransmitting and neuroendocrine neurons remains unknown.

Transcription factors are implicated in the cell biology of neuropeptides. For example, cAMP response element binding protein (CREB) was originally described as a cAMP-dependent transcriptional stimulator for somatostatin (2). Furthermore, transcriptional networks specify peptidergic neurons in *Drosophila* and mammals (e.g., 3–9). Finally, accumulation of amidated neuropeptides and DCVs in *Drosophila* neurons is enhanced by the transcription factor Dimmed (DIMM) (10–13). Indeed, DIMM induces DCVs in photoreceptors that do not normally possess these organelles (13). Given this history, it is apparent that presynaptic neuropeptide accumulation depends on transcriptionally regulated biosynthesis, which in turn dictates delivery of neuropeptide-containing DCVs by anterograde axonal transport to terminals. However, the hypothesis that neuron-specific variation in presynaptic neuropeptide stores relies on differential DCV delivery to terminals has not been tested.

Drosophila is an advantageous system for approaching this problem. First, as noted above, genetic control of neuropeptide expression has been studied extensively. Second, terminals specialized for cotransmission and neuroendocrine release, which arise from different neurons, have been identified in the periphery: neuromuscular junction type Ib boutons possess an abundance of SSVs and relatively few DCVs, whereas type III boutons contain an abundance of DCVs that contain ecdysis-associated neuropeptides and few SSVs (14–16). Strikingly, type III bouton neuropeptide stores are nearly exhausted following ecdysis (16). Finally, in vivo imaging of GFP-tagged neuropeptides in *Drosophila* nerve terminals has resolved DCV delivery to and capture in boutons (17, 18). Therefore, live imaging of type Ib and III boutons offers the opportunity to test whether dramatic differences in DCV numbers in identified terminals are produced as a consequence of DCV delivery.

Here it is shown that neuropeptide release is proportional to presynaptic neuropeptide storage in type Ib and III boutons, thus illustrating the impact of the dramatic difference in DCV abundance in identified terminals. However, the delivery of neuropeptide-containing DCVs to these boutons is surprisingly similar. Therefore, experiments are performed to identify the basis for differential accumulation of neuropeptide-containing DCVs in these cotransmitting and neuroendocrine nerve terminals.

Results

Consistent with qualitative detection of DCVs by electron microscopy, fluorescence imaging of a transgenic GFP-tagged neuropeptide [preproANF-EMD (emerald GFP), here called Anf-GFP]

Significance

Neuropeptides, which affect mood and behavior, are synthesized in the soma and delivered to nerve terminals for storage and release. Yet, among identified neurons, there is great variation in the abundance of neuropeptides in terminals. Demonstrated transcriptional regulation of neuropeptide synthesis supports the view that presynaptic neuropeptide stores are proportional to synthesis-driven delivery of neuropeptide-containing vesicles to terminals. However, we show that nerve terminals with dramatically different neuropeptide stores are supported by identical vesicle delivery and differ instead in efficiency of vesicle capture. Vesicle capture in the terminal is under transcriptional control and influences vesicle distribution and replacement as well as neuropeptide accumulation for release. Thus, vesicle capture is a major determinant of nerve terminal function.

Author contributions: D.B. and E.S.L. designed research; D.B. performed research; C.Z., R.S.H., and D.L.D. contributed new reagents/analytic tools; D.B. and E.S.L. analyzed data; and D.B. and E.S.L. wrote the paper.

The authors declare no conflict of interest.

This article is a PNAS Direct Submission.

[1]To whom correspondence should be addressed. E-mail: elevitan@pitt.edu.

driven by a panneuronal driver shows greater accumulation of neuropeptide in *Drosophila* type III boutons on muscle 12 than in type Ib boutons of the muscle 6/7 synapse (19). Panneuronal expression is not convenient for studying type III boutons, however, because of the presence of closely apposed type Ib, Is, and II boutons, which arise from different neurons. Therefore, to generate a basis of comparison with type Ib boutons, Anf-GFP expression was induced specifically in type III boutons with the driver *ccap-GAL4* (20), and neuropeptide fluorescence was quantified with wide-field microscopy. These measurements demonstrated sevenfold more neuropeptide in typical spindle-shaped type III boutons than in type Ib boutons (Fig. 1 *A* and *B*). Next, the impact of this dramatic difference on release was determined. To avoid the confound of variation in axon excitability affecting responses to electrical nerve stimulation, release was evoked by depolarization of boutons by replacement of extracellular Na^+ with K^+. In principle, release might vary between boutons for a variety of reasons (e.g., differences in Ca^{2+} channels, the secretory apparatus, or presynaptic neuropeptide stores). However, release efficiency measured as the percentage decrease in fluorescence was identical in type Ib and III boutons (Fig. 1*C*) suggesting that differences are most simply explained by neuropeptide release being scaled in proportion to presynaptic neuropeptide stores.

Therefore, the basis for the greater presynaptic neuropeptide store found in type III boutons was investigated. First, because differences in neuropeptide accumulation could reflect the number of DCVs and their individual content, the fluorescence of single GFP puncta likely to be individual DCVs (17) was measured in axons near the most proximal type Ib and III boutons. Interestingly, individual DCV fluorescence (F_{DCV}) was 22% less in single type III axon DCVs (Fig. 1*D*). A calculation of normalized bouton fluorescence divided by single DCV fluorescence (F_{bouton}/F_{DCV}) revealed that there are 9.2-fold more DCVs in type III boutons than in type Ib boutons.

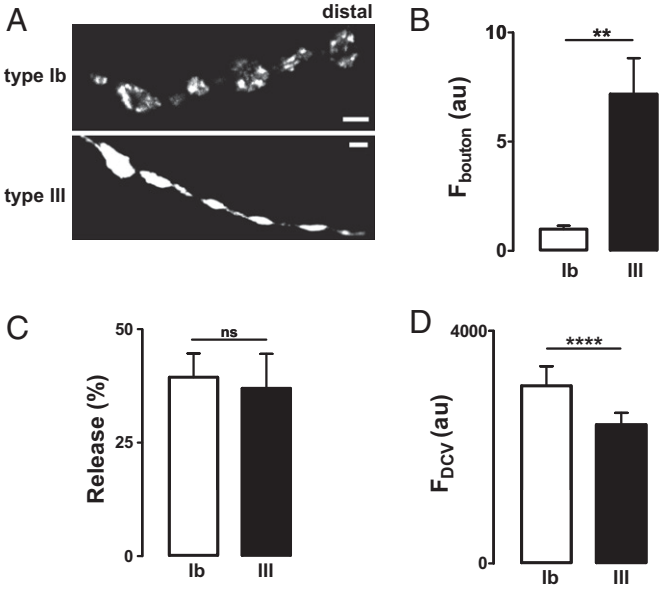

Fig. 1. Type Ib and type III boutons differ in neuropeptide content and DCV number. (*A*) Images of type Ib (*Upper*) and type III (*Lower*) boutons expressing Anf-GFP. (Scale bars, 2 μm.) (*B*) Neuropeptide fluorescence per bouton (F_{bouton}) of type Ib ($n = 16$) and type III boutons ($n = 20$) in arbitrary units (au). $^{**}P < 0.01$. (*C*) Depolarization-evoked neuropeptide release in type Ib ($n = 8$) and type III boutons ($n = 4$) measured as the percent decrease in fluorescence. ns, not significant. Boutons were stimulated with elevated extracellular K^+ for 3 min. (*D*) Single DCV fluorescence in axons leading to type Ib ($n = 56$) and type III boutons ($n = 53$). $^{****}P < 0.0001$. Error bars represent SEM.

The simplest explanation for the difference in DCV number would be that more neuropeptide-containing DCVs are made and thus supplied by anterograde axonal transport to type III boutons than to type Ib boutons. Therefore, the flux of DCVs (i.e., the number traveling through a specific area) was measured in axons proximal to the first type III and Ib boutons in the absence of Ca^{2+} to prevent release. Surprisingly, anterograde axonal transport was the same in type Ib and III bouton axons (Fig. 2*A*), implying that the difference in DCV number is not explained by synthesis-driven supply from the soma.

In both bouton types, steady-state anterograde and retrograde flux were similar (Fig. 2*A*) suggesting that terminal DCV numbers were at steady state. Therefore, a difference in DCV turnover could provide an alternative explanation for the number of DCVs in type III and Ib boutons. Previously, fluorescence recovery after photobleaching (FRAP) showed that type Ib DCVs have a half-life of ~6 h (17). Therefore, half-life would have to be ~55 h in type III boutons to account for their greater DCV number. However, FRAP at 0.5 and 1 h in type III boutons (Fig. 2*B*) was not different from published for type Ib bouton results (17). Independent verification of similar turnover was obtained with the use of the fluorescent timer protein monomeric Kusabira Green Orange (mK-GO), which transitions from green to red fluorescence with age (21). As this color transition is half-maximal at 6 h and occurs inside DCVs (21), Anf tagged with mK-GO was expressed in *Drosophila*. If DCV half-life differed in type Ib and III boutons, this should be evident as a difference in age measured as the ratio of green to red mK-GO–tagged Anf. However, this ratio was similar in type Ib and III boutons (Fig. 2 *C* and *D*). Therefore, there is no experimental evidence that the greater number of DCVs in type III boutons is explained by slower turnover.

As delivery and turnover were not sufficient to account for differences in DCV number, DCV capture in the two bouton types was compared. In type Ib motoneurons, DCVs circulate over long distances based on inefficient sporadic capture so that neuropeptide accumulates equivalently across en passant boutons (18) and there is a pool of circulating DCVs that can be tapped into by activity-dependent capture to rapidly replenish neuropeptide stores following release (17). One indicator of inefficient capture is that FRAP is initially most marked in the most distal Ib bouton (Fig. 3*A*, *Left*) because many DCVs transit through proximal boutons without being captured (18). Therefore, we investigated whether a similar pattern is found in type III boutons. Importantly, FRAP was very different: neuropeptide accumulation was initially most marked in proximal boutons with little traffic reaching the most distal boutons (Fig. 3*A*, *Right*). Consistent with the supply of DCVs dropping precipitously as DCVs pass through en passant type III boutons, the most distal bouton in type III synapses was always small, whereas it is usually comparable to or even larger than proximal en passant boutons in type Ib synapses (Figs. 1*A* and 3*A*). To further evaluate this difference, anterograde flux into and out of type III boutons was quantified. Although this flux drops only ~10% per type Ib bouton (18), a ~65% drop in flux is found in proximal type III boutons, showing that capture efficiency is dramatically greater (Fig. 3*B*). Such efficient capture would leave few DCVs to circulate and so compromise the source of DCVs that supports activity-dependent capture. In accordance with this prediction, the rebound in presynaptic neuropeptide content following release that is produced by activity-dependent capture in type Ib boutons (17) is absent in type III boutons (Fig. 3*C*). Together, these results show that constitutive DCV capture efficiency is much higher in type III boutons leading to greater presynaptic neuropeptide accumulation, albeit at the expense of distal distribution and rapid replenishment following robust release.

The transcription factor DIMM regulates the capacity to accumulate amidated neuropeptide-containing DCVs in a subpopulation (~3%) of *Drosophila* neurons without regulating

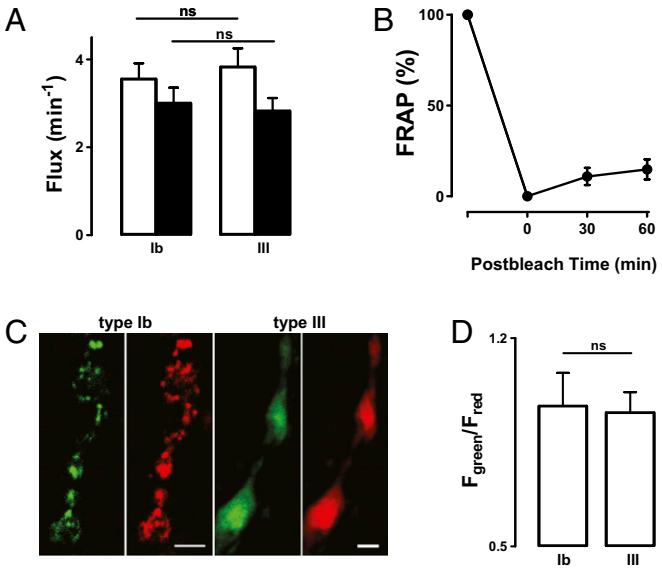

Fig. 2. DCV transport and turnover are similar in type Ib and type III boutons. (*A*) Anterograde (open bars) and retrograde (filled bars) DCV flux at proximal type Ib ($n = 19$) and type III boutons ($n = 23$). ns, not significant. (*B*) The percent FRAP over time following photobleaching in type III boutons ($n = 4$). (*C*) Age-dependent labeling of DCVs expressing Anf tagged with mK-GO in type Ib and III boutons. For each bouton type, green (young) and red (old) images are shown side by side. (Scale bars, 2 μm.) (*D*) Ratio of green to red fluorescence in type Ib ($n = 8$) and type III boutons ($n = 10$).

neuropeptide gene expression (10–13, 22). Although this could be assumed to reflect an effect on DCV synthesis that is not cargo-specific, the above results from type Ib and III boutons suggested the alternative possibility that DIMM promotes DCV capture. DIMM is not present in the third instar neurons studied here, thus ruling out knockdown experiments. However, it was possible to test the hypothesis that DIMM boosts DCV capture in type Ib boutons, which had not been examined in previous DIMM studies. Specifically, because global expression of DIMM is lethal, *eveRRA-Gal4* (23) was used to drive Anf-GFP and DIMM expression in the anterior corner cell (aCC) motoneuron, which produces the type Ib bouton terminal on muscle 1. Consistent with previous studies of ectopic neuropeptide expression (10), DIMM dramatically increased accumulation of presynaptic Anf-GFP (Fig. 4 *A* and *B*). Also, boutons became more spindle-shaped (i.e., a morphology more similar to type III boutons) (Fig. 4 *A* and *B*). As individual DCVs were not detectable in these single cross animals, FRAP experiments were performed to assess capture efficiency. Consistent with muscle 6/7 Ib terminals (Fig. 3*A*), distal polarized accumulation of Anf-GFP was seen in muscle 1 type Ib boutons (Fig. 4*B*, *Left*). However, upon expression of DIMM, the distal bias that is indicative of inefficient capture was lost (Fig. 4*B*, *Right*). Quantification verified that DIMM altered FRAP to make it more similar to type III boutons (Fig. 4*C*). Thus, a transcription factor that increases neuropeptide accumulation enhances presynaptic DCV capture.

Discussion

Nerve terminals vary in their content of neuropeptide-containing DCVs, which determines the capacity for cotransmission or neuroendocrine function. For decades, molecular studies focused on the role of transcriptional regulation in controlling neuropeptide gene expression. Thus, it was easy to assume that presynaptic neuropeptide accumulation is determined by synthesis that in turn dictates delivery to nerve terminals. According to this view, large presynaptic neuropeptide stores are maintained by scaled-up production and anterograde axonal transport of DCVs. However, here it was shown that dramatically different DCV numbers in *Drosophila* type Ib and III boutons are associated with similar axonal transport. Turnover, which affects steady-state levels, and individual DCV content are also comparable. Surprisingly, it is efficiency of DCV capture that distinguishes neuropeptide storage and hence the capacity for release by these cotransmitting and neuroendocrine terminals.

Taking into account neuron-specific variation in presynaptic DCV capture, what is the role of previously studied transcriptional control? First, differentially regulating synthesis may allow distinct neuropeptides to compete for packaging in DCVs. As newly made peptides can be released preferentially (21, 24), transcriptional regulation that alters DCV content can change the mixture of neuropeptides released at the nerve terminal. Second, DCV capture is itself increased by the transcription factor DIMM, which was known to increase the accumulation of neuropeptide-containing DCVs in central neurons (10, 13). Presumably, DIMM induces a gene encoding for a presynaptic DCV capture effector, which might be regulated by kinases and G proteins (25, 26). Importantly, the demonstration of genetic regulation of DCV capture clarifies why multiple transcription factors including DIMM specify individual peptidergic neurons in *Drosophila* (4–6, 9): DCV capture and the synthesis of specific DCV cargoes are independently controlled to determine presynaptic neuropeptide accumulation. Although neuropeptide synthesis was not measured here, neuron-specific capture was shown to be an important target of the complex transcriptional networks that control peptidergic function.

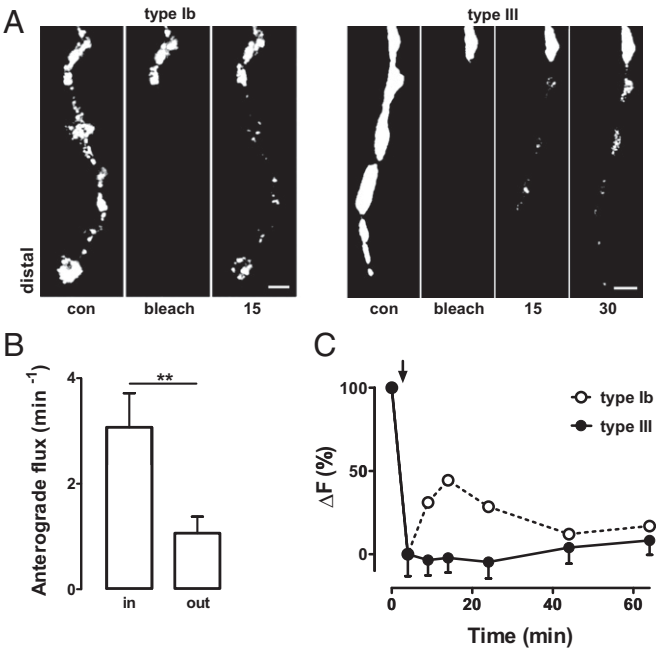

Fig. 3. DCV capture in type III boutons is efficient. (*A*) Time-lapse images of type Ib and type III boutons before and after photobleaching boutons. FRAP shows DCV accumulation is marked in the most distal type Ib boutons and the most proximal type III boutons. Contrast was adjusted to visualize puncta. Numbers indicate time in minutes. Proximal unbleached boutons are shown at the top of images. (Scale bar, 2 μm.) (*B*) DCV anterograde flux into and out of photobleached proximal type III boutons shows high capture efficiency in type III boutons ($n = 7$). $^{**}P < 0.01$. (*C*) Change in neuropeptide content after a 3-min depolarization (indicated by arrow) of type III boutons (black circles) ($n = 8$). Data are normalized to the initial decrease in fluorescence (ΔF). Dotted curve (open circles) shows the rebound in type Ib boutons (replotted from ref. 17) evoked by the same stimulus that is indicative of activity-dependent DCV capture.

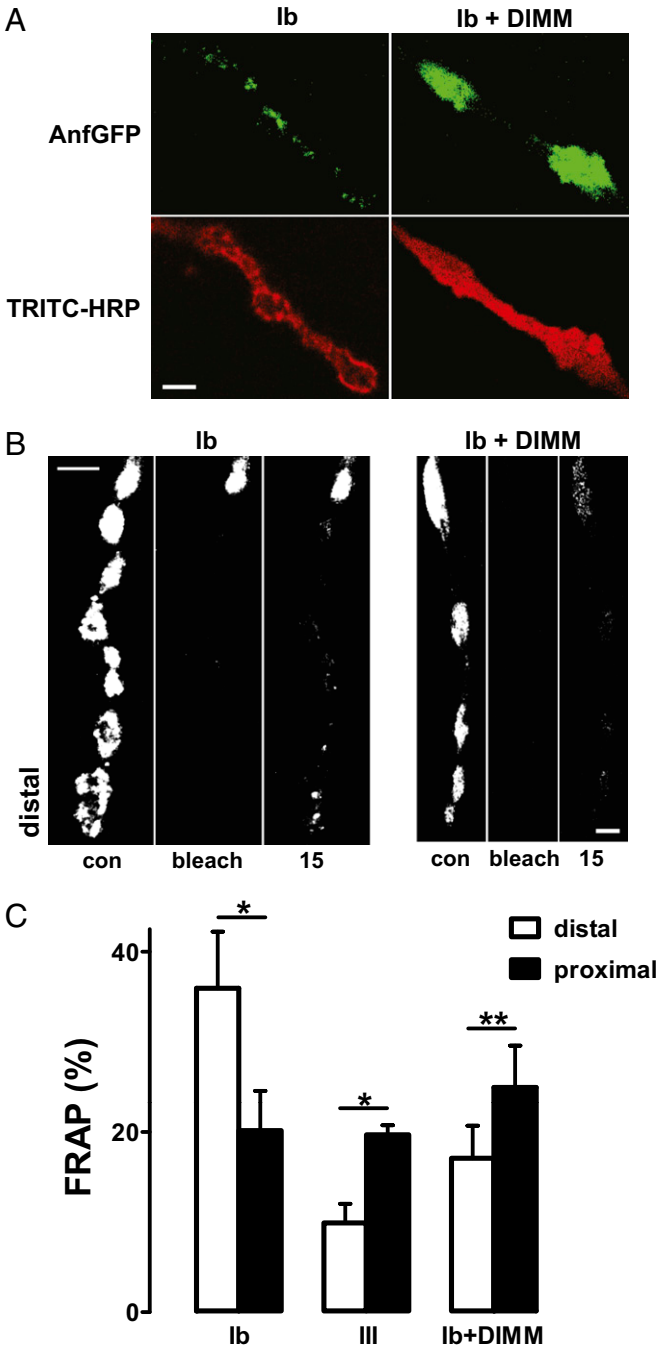

Fig. 4. DIMM confers peptidergic type III bouton properties onto type Ib boutons. (*A*) Fluorescent images of type Ib boutons on muscle 1 in wild-type (*Left*) and DIMM-expressing (*Right*) flies. (*Upper*) Anf-GFP in green. (*Lower*) The same boutons stained with TRITC-HRP antibody (red) to reveal presynaptic morphology. (*B*) FRAP measured as percent recovery in 15 min for muscle 1 type Ib boutons with and without DIMM. Note the switch from distal to proximal recovery. (Scale bars, 2 μm.) (*C*) Quantification of FRAP in muscle 1 type Ib boutons ($n = 5$), type III boutons ($n = 8$), and type Ib boutons expressing DIMM ($n = 6$). $*P < 0.05$, $**P < 0.01$.

Interestingly, efficient presynaptic DCV capture maximizes neuropeptide release, but this benefit comes with tradeoffs. First, efficient capture biases DCV delivery to proximal boutons. This is a hindrance to neurons that must innervate multiple targets at different distances from the soma and neurons that have many en passant boutons to supply (e.g., there are far more muscle 6/7 type Ib boutons than muscle 12 type III boutons). For these cases, equal distribution of resources by vesicle circulation and sporadic capture (18) is more suitable. Second, efficient capture might hinder extension of the terminal because few vesicles avoid capture in proximal boutons to reach the distal end of the terminal. Indeed, proximal capture may account for the finding reported here that the most distal type III bouton is small, which is not the case for type Ib boutons. Finally, with efficient constitutive capture, DCVs are not replaced quickly following intense release as there are relatively few circulating vesicles to replenish acutely depleted stores. Instead, DCV flux is dominated by steady-state supply and removal of DCVs. The resultant slow replacement of released neuropeptides is not a problem for neuroendocrine type III boutons because, although release nearly empties neuropeptide stores at ecdysis (16), this developmental behavior occurs only four times in the life of *Drosophila*. It is conceivable that these boutons release at other times as well, but as long as such responses are modest, replenishment will not be limiting given their substantial neuropeptide stores. However, this is not desirable for dynamic cotransmitting boutons. In the latter case, inefficient capture is preferable as fewer DCVs are needed for release, and activity-dependent capture of circulating vesicles rapidly replaces depleted stores (17, 18). The widespread impact on neuropeptide distribution, release, and replacement clarifies why presynaptic DCV capture is an effective control point for neuron-specific peptidergic function.

Materials and Methods

Flies. Muscle 6/7 synapse type Ib boutons were studied in Figs. 1–3 with elav-GAL4 UAS-Anf-GFP larvae (19). Type III boutons were studied in upstream activating sequence (*UAS*)-*Anf-GFP; ccap-GAL4* larvae. For Fig. 4, muscle 1 type Ib boutons were studied in a recombinant of *eveRRA-GAL4 UAS-Anf-GFP* on chromosome 3 (27; kindly provided by C. Collins). In Fig. 4*A*, this line was crossed to Canton S flies for a wild-type control or *UAS-DIMM* flies (kindly provided by P. Taghert). Several independent chromosomal insertions of *UAS-DIMM* gave similar results (i.e., a marked increase in neuropeptide content). For FRAP experiments on muscle 1, it was desirable to minimize differences in total neuropeptide expression. Therefore, homozygous *eveRRA-GAL4 UAS-Anf-GFP* larvae were compared with single cross with UAS-DIMM. To generate a timer line, the ANF gene was excised from the ANF-pEGFP-N1 construct (28) by cutting with EcoRI/KpnI, and the mK-GO gene from the neuropeptide Y-mK-GO construct [20; kindly provided by A. Miyawaki of The Institute of Physical and Chemical Research (Japan) (RIKEN) and T. Tsuboi of the University of Tokyo] was amplified by PCR with linkers containing the KpnI site in forward primer and NotI site in reverse primer. Following cutting with KpnI and NotI, ANF and mK-GO were cloned into the PC5-Kan vector. Then ANF-mK-GO was excised and cloned into the pUAS-C5, which was used to generate transgenic flies by Bestgene, Inc. Expression was driven with Ok6-GAL4.

Imaging. Protocols for wide-field microscopy and FRAP have been described previously (17, 18, 29). Briefly, filleted third instar larvae were viewed with an Olympus 60× 1.1 numerical aperture objective. For K^+-induced depolarization, the NaCl in the extracellular solution (HL3: 70 mM NaCl, 5 mM KCl, 1.5 mM $CaCl_2$, 20 mM $MgCl_2$, 10 mM $NaHCO_3$, 5 mM trehalose, 115 mM sucrose, 5 mM sodium Hepes, pH 7.2) was replaced with KCl. For constitutive traffic, the Ca^{2+} in HL3 was substituted with 0.5 mM Na_3 EGTA to prevent release. FRAP was performed with an Olympus Fluoview 1000 scanning laser confocal microscope. Wide-field imaging used Hamamatsu cooled ccd cameras. Standard fluorescein optics were used for imaging GFP. In mK-GO experiments, excitation was switched between 488- and 561-nm lasers with simultaneous switching between green bandpass and red long-pass filters. The mK-GO ratio depends on microscope optics and increases to its half-maximal value in 6 h (21), which is similar to the half-life of DCVs in type Ib boutons (17). Statistical significance was calculated with the *t* test.

ACKNOWLEDGMENTS. We thank T. Tsuboi (University of Tokyo) and A. Miyawaki (RIKEN) for the mK-GO–tagged Neuropeptide Y plasmid, C. Collins (University of Michigan) for eveRRA-GAL4 UAS-Anf-GFP flies, and P. Taghert (Washington University in St. Louis) for UAS-DIMM flies. This research was supported by National Institutes of Health Grant R01 NS32385.

1. Taghert PH, Nitabach MN (2012) Peptide neuromodulation in invertebrate model systems. *Neuron* 76(1):82–97.
2. Montminy MR, Bilezikjian LM (1987) Binding of a nuclear protein to the cyclic-AMP response element of the somatostatin gene. *Nature* 328(6126):175–178.
3. Benveniste RJ, Thor S, Thomas JB, Taghert PH (1998) Cell type-specific regulation of the *Drosophila* FMRF-NH2 neuropeptide gene by Apterous, a LIM homeodomain transcription factor. *Development* 125(23):4757–4765.
4. Allan DW, Park D, St Pierre SE, Taghert PH, Thor S (2005) Regulators acting in combinatorial codes also act independently in single differentiating neurons. *Neuron* 45(5):689–700.
5. Allan DW, St Pierre SE, Miguel-Aliaga I, Thor S (2003) Specification of neuropeptide cell identity by the integration of retrograde BMP signaling and a combinatorial transcription factor code. *Cell* 113(1):73–86.
6. Miguel-Aliaga I, Thor S, Gould AP (2008) Postmitotic specification of *Drosophila* insulinergic neurons from pioneer neurons. *PLoS Biol* 6(3):e58.
7. Huang M, et al. (2008) Ptf1a, Lbx1 and Pax2 coordinate glycinergic and peptidergic transmitter phenotypes in dorsal spinal inhibitory neurons. *Dev Biol* 322(2):394–405.
8. Xu Y, et al. (2008) Tlx1 and Tlx3 coordinate specification of dorsal horn pain-modulatory peptidergic neurons. *J Neurosci* 28(15):4037–4046.
9. Eade KT, Fancher HA, Ridyard MS, Allan DW (2012) Developmental transcriptional networks are required to maintain neuronal subtype identity in the mature nervous system. *PLoS Genet* 8(2):e1002501.
10. Hewes RS, Park D, Gauthier SA, Schaefer AM, Taghert PH (2003) The bHLH protein Dimmed controls neuroendocrine cell differentiation in *Drosophila*. *Development* 130(9):1771–1781.
11. Park D, et al. (2008) The Drosophila basic helix-loop-helix protein DIMMED directly activates PHM, a gene encoding a neuropeptide-amidating enzyme. *Mol Cell Biol* 28(1):410–421.
12. Park D, Veenstra JA, Park JH, Taghert PH (2008b) Mapping peptidergic cells in Drosophila: where DIMM fits in. *PLoS ONE* 3(3):e1896.
13. Hamanaka Y, et al. (2010) Transcriptional orchestration of the regulated secretory pathway in neurons by the bHLH protein DIMM. *Curr Biol* 20(1):9–18.
14. Atwood HL, Govind CK, Wu CF (1993) Differential ultrastructure of synaptic terminals on ventral longitudinal abdominal muscles in *Drosophila* larvae. *J Neurobiol* 24(8): 1008–1024.
15. Jia XX, Gorczyca M, Budnik V (1993) Ultrastructure of neuromuscular junctions in *Drosophila*: comparison of wild type and mutants with increased excitability. *J Neurobiol* 24(8):1025–1044.
16. Loveall BJ, Deitcher DL (2010) The essential role of bursicon during *Drosophila* development. *BMC Dev Biol* 10:92.
17. Shakiryanova D, Tully A, Levitan ES (2006) Activity-dependent synaptic capture of transiting peptidergic vesicles. *Nat Neurosci* 9(7):896–900.
18. Wong MY, et al. (2012) Neuropeptide delivery to synapses by long-range vesicle circulation and sporadic capture. *Cell* 148(5):1029–1038.
19. Rao S, Lang C, Levitan ES, Deitcher DL (2001) Visualization of neuropeptide expression, transport, and exocytosis in *Drosophila* melanogaster. *J Neurobiol* 49(3):159–172.
20. Hodge JJ, Choi JC, O'Kane CJ, Griffith LC (2005) Shaw potassium channel genes in *Drosophila*. *J Neurobiol* 63(3):235–254.
21. Tsuboi T, Kitaguchi T, Karasawa S, Fukuda M, Miyawaki A (2010) Age-dependent preferential dense-core vesicle exocytosis in neuroendocrine cells revealed by newly developed monomeric fluorescent timer protein. *Mol Biol Cell* 21(1):87–94.
22. Park D, et al. (2011) Molecular organization of *Drosophila* neuroendocrine cells by Dimmed. *Curr Biol* 21(18):1515–1524.
23. Fujioka M, et al. (2003) Even-skipped, acting as a repressor, regulates axonal projections in *Drosophila*. *Development* 130(22):5385–5400.
24. Duncan RR, et al. (2003) Functional and spatial segregation of secretory vesicle pools according to vesicle age. *Nature* 422(6928):176–180.
25. Wong MY, Shakiryanova D, Levitan ES (2009) Presynaptic ryanodine receptor-CamKII signaling is required for activity-dependent capture of transiting vesicles. *J Mol Neurosci* 37(2):146–150.
26. Wu YE, Huo L, Maeder CI, Feng W, Shen K (2013) The balance between capture and dissociation of presynaptic proteins controls the spatial distribution of synapses. *Neuron* 78(6):994–1011.
27. Ghannad-Rezaie M, Wang X, Mishra B, Collins C, Chronis N (2012) Microfluidic chips for in vivo imaging of cellular responses to neural injury in *Drosophila* larvae. *PLoS ONE* 7(1):e29869.
28. Burke NV, et al. (1997) Neuronal peptide release is limited by secretory granule mobility. *Neuron* 19(5):1095–1102.
29. Levitan ES, Lanni F, Shakiryanova D (2007) In vivo imaging of vesicle motion and release at the *Drosophila* neuromuscular junction. *Nat Protoc* 2(5):1117–1125.